AGU PUBLICATIONS

Geophysical Research Letters

RESEARCH LETTER
10.1002/2017GL074959

Key Points:
- Eclogitizied Hess Rise conjugate induces a rapid subsidence in the Gulf of Mexico during the Paleocene
- Heterogeneous buoyancy in the subducted Farallon slab caused by the eclogitizied Hess conjugate tilts the surface southward
- Presently, the predicted Hess conjugate localizes below the northern GOM, which coincides with a seismic anomaly in mantle

Supporting Information:
- Supporting Information S1

Correspondence to:
H. Wang,
huilin@gps.caltech.edu

Citation:
Wang, H., Gurnis, M., & Skogseid, J. (2017). Rapid Cenozoic subsidence in the Gulf of Mexico resulting from Hess Rise conjugate subduction. *Geophysical Research Letters*, *44*, 10,930–10,938. https://doi.org/10.1002/2017GL074959

Received 17 JUL 2017
Accepted 13 OCT 2017
Accepted article online 20 OCT 2017
Published online 11 NOV 2017

Rapid Cenozoic Subsidence in the Gulf of Mexico Resulting From Hess Rise Conjugate Subduction

Huilin Wang[1], Michael Gurnis[1], and Jakob Skogseid[2]

[1]Seismological laboratory, California Institute of Technology, Pasadena, CA, USA, [2]Statoil ASA, Fornebu, Norway

Abstract Enigmatic surface deflections occurred in North America starting from the Cretaceous, including the continental-scale drainage reorganization and the long-wavelength subsidence in the Western Interior Seaway. These surface undulations cannot be simply explained by sea level change or flexure loading. Coinciding with the large-scale surface deflection, the Gulf of Mexico (GOM) has an immense Paleocene sediment deposition probably caused by tectonic subsidence. Increasing evidence indicates a distinct seismic anomaly localized in the mantle below the GOM. With geodynamic models, we show that the Hess Rise conjugate coincides with the position of the seismic anomaly. The basalt-eclogite transition in the Hess conjugate can lead to a localized dynamic subsidence in the GOM, which is superimposed on the broad surface deflection caused by the Farallon slab. The Hess conjugate, transformed to eclogite, could tilt the surface southward in the U.S. and help frame the GOM as a main depocenter in the Cenozoic.

1. Introduction

The Gulf of Mexico, an important hydrocarbon-bearing basin in North America, has undergone multiple stages of subsidence and sedimentation (Figure 1). It formed by Mesozoic rifting and crustal extension, followed by Pangea breakup and Late Jurassic-Early Cretaceous seafloor spreading (Pindell, 1985; Salvador, 1991). Thermal cooling and sediment loading are believed to be the causal mechanisms for the subsidence in the deep Gulf of Mexico (GOM) (Galloway, 1989). However, substantially after the rifting period, an additional isolated subsidence occurred in the GOM. A backstripping analysis of the deep GOM suggests the tectonic subsidence deviated from the slow thermal-cooling-induced subsidence by ~2 km at some time in the Late Cretaceous or the Cenozoic (Feng et al., 1994) (Figure 1c). Contemporaneously, the deposition rate profoundly increased in the GOM in the Paleocene, which is ~3 times the Cenozoic average (Galloway et al., 2011) (Figure 1c). More intriguing, a lateral variation of sediment thickness in Cenozoic strata indicates an eastward migration of the depocenter in the GOM (Galloway, 2008) (Figure 1d). Before the Paleocene, the sediment thickness was almost uniform (Feng et al., 1994). But the Paleocene basin fill (sand-rich lower Wilcox Group) was mainly deposited in the west, then the center of basin infill gradually shifted eastward in the Neogene and Quaternary. One explanation for the enigmatic subsidence in the GOM is flexure-induced loading from the Laramide orogeny (Feng et al., 1994). However, the Laramide orogeny loading cannot explain the eastward migration of sedimentation in the GOM through the Cenozoic.

On a continental scale, several observations point to a large-scale change in the surface topography of North America starting in the Cretaceous, including continental-scale drainage reorganization with a shift in the depocenters and the formation of the Western Interior Seaway. Before the dramatic surface deflection, river networks from the Rocky Mountain fold and thrust belt to the Appalachian Mountains were flowing northeast to the Boreal Sea. Only a small part of the southern U.S. was shedding sediments to the GOM. But from the Maastrichtian to the Paleocene, the main routing direction in the U.S. changed from northward to southward (Blum & Pecha, 2014). Sediments from the Western Cordillera to the Appalachian Mountains were transported to the GOM (Galloway et al., 2011). In addition, the development of the Western Interior Seaway began in the Aptian. About 40% of the continent experienced marine inundation in the Late Cretaceous with >1 km of marine sediments deposited (e.g., DeCelles, 2004 ; Smith et al., 1994). Bond (1976) estimated that the flooding area requires ~310 m of sea level rise and provides room for ~700 m of sediments, which is much less than the observed thickness of Late Cretaceous strata. A more detailed analysis of the marine sediments shows that the depocenter initially resided in the foreland basin in the region of Utah and then migrated eastward to Wyoming and Colorado during the Late Cretaceous (DeCelles, 2004). During the Paleocene, the seaway retreated in the continental interior but still prevailed around the GOM.

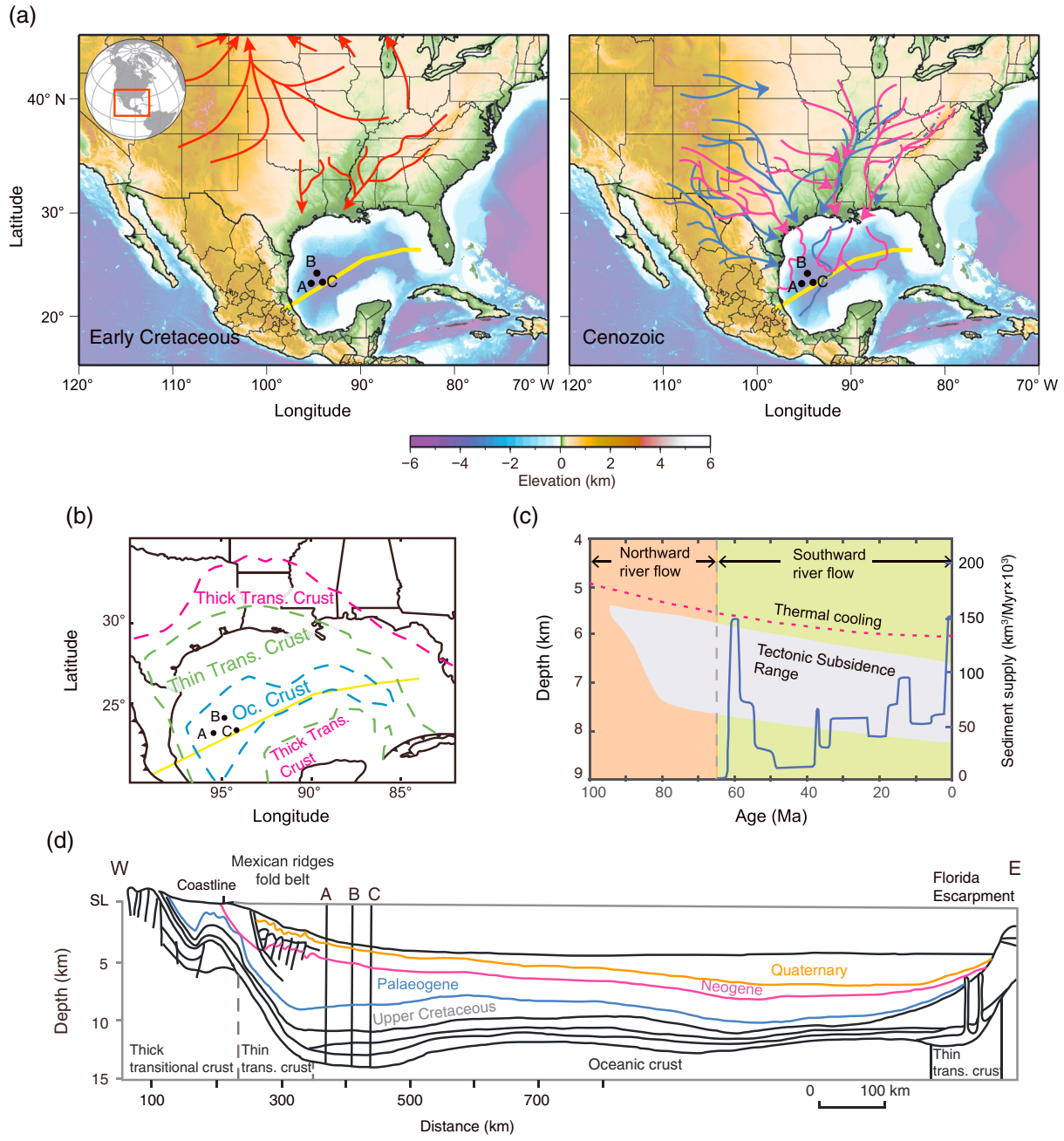

Figure 1. (a) Surface topography and paleo-drainage system. The left plot shows the river network in the early Cretaceous (Blum & Pecha, 2014). The right plot shows the evolution of drainage system in the Cenozoic. The blue and magenta lines indicate paleo-river systems and the depocenter extent in the GOM in the Paleogene and Middle Miocene, respectively (Galloway et al., 2011). The black dots (A, B, and C) represent borehole locations. (b) Crustal types in the GOM. The deep, central part of the Gulf of Mexico basin is underlain by basaltic oceanic crust and filled by generally undeformed Mesozoic and Cenozoic sediments (Salvador, 1991). The thick and thin transitional (trans.) continental crusts were stretched by Jurassic rifting (Galloway, 2008). (c) Subsidence in the GOM. The grey shaded area is the range of tectonic subsidence derived from backstripping analysis for locations A, B, and C (Feng et al., 1994) (see Figures 1a and 1b for locations). The red dashed line shows theoretical thermal subsidence for a 50–150 Myr old oceanic crust (Parsons & Sclater, 1977). The blue line shows the volume of sediment supply in the GOM during the Cenozoic (Galloway et al., 2011). (d) Cross section showing sediment strata (Feng et al., 1994). The orientation of cross section is shown in the yellow line (in Figures 1a and 1b).

The enigmatic surface evolution in North America cannot be simply explained by sea level change or orogenic loading/foreland flexure (e.g., Cross & Pilger, 1978; Liu & Nummedal, 2004 ; Painter & Carrapa, 2013). Instead, mantle stresses have been used to interpret the temporal surface deflection. The broad surface deflections in North America approximately correlate with the time and space of dynamic topography

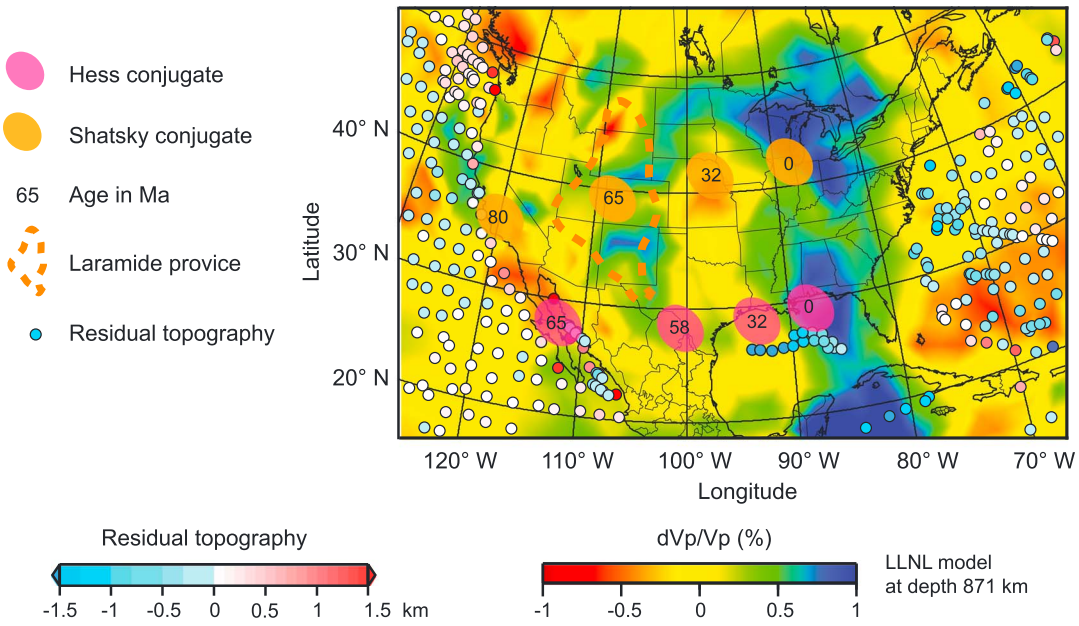

Figure 2. Geophysical observations for North America with the predicted locations of the Hess (purple ellipses) and Shatsky conjugates (orange ellipses) from numerical models. The background is the LLNL-G3Dv3 tomography image at a depth of 871 km (Simmons et al., 2012). The residual depth anomalies are shown with circles (Hoggard et al., 2016). The orange dashed line shows the extent of Laramide province (DeCelles, 2004).

generated by the subducted Farallon plate (Liu et al., 2008; Mitrovica et al., 1989; Spasojević et al., 2009). The GOM could record this dynamic topography signal. However, the ~2 km tectonic subsidence in the GOM is deeper and more localized than the dynamic topography signal that normally has an amplitude of several hundred meters over a wavelength of several thousand kilometers (e.g., Gurnis et al., 1998). The surface can subside more (up to 1 km) when the slab is at shallow depths (e.g., a flat or shallow-dipping slab) (Gurnis, 1992; Heller & Liu, 2016; Mitrovica et al., 1989). But the GOM is ~1,000 km away from the trench and there is little evidence for a period of flat-slab subduction affecting the GOM. Therefore, a different force is needed to explain the GOM dynamics.

Increasing evidence indicates a compositionally distinct anomaly in the mantle below the GOM, which may have contributed to the geological evolution. Seismic tomography shows three high-velocity patches at ~871 km below the Great Lakes, the northern GOM, and the Caribbean (Simmons et al., 2012) (Figure 2). The seismic anomaly below the northern GOM is characterized by sharp boundaries with a seismic shear-wave velocity anomaly (δV_s) elevated by 2.5% over a 50 km distance (Ko et al., 2017). This sharp seismic gradient cannot be explained by a cold Farallon slab, as thermal diffusion would reduce the gradient of δV_s by ~7 times from that observed. Therefore, the high compressional wave seismic velocities may indicate a distinct composition.

The mantle anomalies below the northern GOM and the Great Lakes are interpreted to be the Hess conjugate and the Shatsky conjugate, respectively (Liu et al., 2010; Sun et al., 2017). The Hess Rise formed along the Pacifica-Farallon ridge at ~110 Ma, with its conjugate on the Farallon plate (Livaccari et al., 1981). The Shatsky Rise formed at the Pacific-Farallon-Izanagi triple junction between ~135 Ma with the conjugate on the Farallon and Izanagi plates (Nakanishi et al., 1999). The Hess and Shatsky Rises are still preserved on the Pacific plate. The oceanic plateaus are characterized by a significant thickness (~20 km) of basaltic crust (Coffin & Eldholm, 1994; Korenaga & Sager, 2012; Vallier et al., 1983). The buoyancy of the thick crust in the Shatsky conjugate might have arisen from a flat slab with basement-involved Laramide deformation in the Late Cretaceous (e.g., Saleeby, 2003). In contrast, the fate of the Hess conjugate has not been discussed but might have subducted as a normal-dipping slab. As the oceanic plateau enters high pressure and temperature fields, the basaltic crust can undergo a basalt-eclogite metamorphic phase transition. Being rich in garnet and omphacite, eclogitizied rocks can be 50–300 kg/m^3 denser than pyrolite mantle (Cloos, 1993; Hacker, 1996). Therefore, the eclogitizied oceanic plateau would be denser than the normal slab and

contribute to the downgoing negative buoyancy of the slab unevenly. Geodynamic studies have investigated the surface evolution caused by the low-temperature slab (Mitrovica et al., 1989; Spasojević et al., 2008), but how the eclogitizied oceanic plateau affects the surface topography is unclear.

Here we investigate the influence of mantle convection on the evolution of sedimentary basins, specifically the enigmatic subsidence in the GOM and its relation with the Hess conjugate. We aim to study the dynamic topography arising from the thermally and compositionally induced (eclogitizied oceanic plateau) buoyancy of the subducted slab.

2. Methods

We compute forward numerical models in a spherical domain, using the finite element code *CitcomS* (Zhong et al., 2000), which solves the equations for the conservation of mass, momentum, and energy with the Boussinesq approximation. Paleogeographical constrains are incorporated into surface velocity fields and the thermal structure of oceanic plates (Bower et al., 2015). This semiempirical approach ensures the spatial and temporal distributions, and the buoyancy of downgoing slabs are consistent with the predictions from plate reconstructions (Bower et al., 2015).

The global mantle convection model has 12 caps, each with $128 \times 128 \times 64$ elements, giving a lateral resolution of ~50 km at the surface and ~28 km at the core-mantle boundary. Refinement is used in the radial direction, providing an average resolution of ~45 km, with ~16 km near surface and lower resolutions at greater depths. The model has a free-slip lower boundary. All materials have a Newtonian viscosity (Table S1 in the supporting information).

The models span the period from 230 Ma to the present. Initial temperature structures are derived from a half-space cooling model based on the synthetic ages of the ocean floor and simplified tectono-thermal ages of continental lithosphere (Flament et al., 2014). To simulate asymmetric subduction, the shallow thermal structure of slabs (above 350 km depth) is assimilated based on the location and polarity of subduction zones with a dip angle of 45°. Below 350 km depth, the slab is merged with the thermal structure of mantle, which evolves dynamically (Bower et al., 2015). To obtain the dynamic topography, we re-solve the Stokes equation with a no-slip surface boundary and eliminate the buoyancy and lateral viscosity above 250 km depth, then scale the radial stress on surface (e.g., Flament et al., 2015).

The Hess and Shatsky conjugates are represented by tracers, in order to track their locations and simulate the density variations induced by the basalt-eclogite phase change. Their positions before subduction are reconstructed based on the age and kinematic motion of the underlying oceanic plate (Figure S1 in the supporting information). As the Hess conjugate subducts to depths greater than 100 km, where the temperature and pressure conditions enter the stability field of eclogite, we increase the density of the upper 20 km of the Hess conjugate to 3500 kg/m^3, which is 200 kg/m^3 denser than ambient mantle. In models, the other properties of plateaus (e.g., rheology) are identical as normal oceanic plates. We aim to investigate the consequences of eclogitizied oceanic plateaus, instead of detailed metamorphic processes.

3. Results

The Farallon plate subducted under the west coast of North America from ~180 Ma. The synthetic Hess conjugate subducted under northern Mexico at ~68 Ma (Figure S1). At ~64 Ma, the Hess conjugate entered the eclogite stability field. We assume the basaltic crust in the Hess conjugate transformed to eclogite and its density increased (Model 1; Table S2). Subsequently, the Hess conjugate descended rapidly compared to the normal oceanic plate in response to its extra density. Presently, the Hess conjugate is located below the northern GOM between 850 and 1150 km depths (Figure 3), which is coincident with the observed seismic anomaly in the mantle (Figure 2).

As the low-temperature Farallon slab subducted, its negative buoyancy depressed the surface and generated a broad topographic low in western-central North America since the Cretaceous (Figure 4). As the North American plate moved westward over the subduced Farallon slab, the dynamic surface low migrated eastward, consistent with earlier studies (e.g., Liu, 2014; Spasojević et al., 2008). Since ~50 Ma, the dynamic topography in western North America gradually uplifted to ~0 km at present.

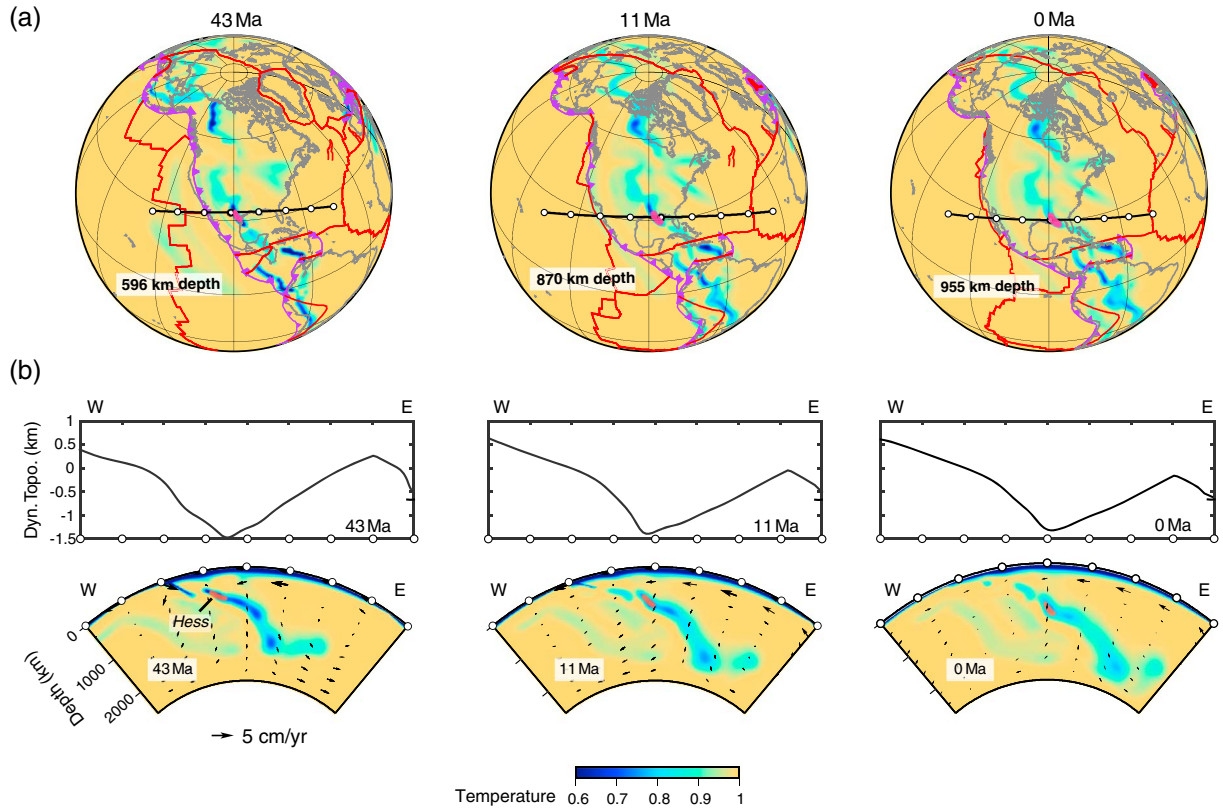

Figure 3. Dynamic topography evolution above the Hess conjugate in the context of hemispheric mantle temperature anomalies. (a) Modeled nondimensional temperature anomaly at the given depths and ages. The red highlighted region around the GOM denotes the location of the Hess conjugate. (b) Cross sections of dynamic topography ("Dyn. Topo."; upper plots) and thermal structures (lower plots) (orientation of profile shown in Figure 3a).

The surface deflection is of greater amplitude in the GOM. Since ~60 Ma, the eclogitizied Hess conjugate migrated beneath the GOM. Because of the extra density, a "bull's-eye"-shaped, deeper surface low is generated above the Hess conjugate (Figure 4a), which has a diameter of ~500 km and the maximum amplitude of ~1.8 km. The eclogitizied Hess conjugate makes the GOM the lowest area in the dynamic topography map of North America. The maximum surface low first entered the western GOM at ~60 Ma, then gradually migrated eastward along the northern GOM. The predicted dynamic surface topography in the western GOM subsides to ~1.3 km by 40–30 Ma, with the most rapid subsidence occurring during 60–50 Ma (Figure 5). After adding the thermal cooling subsidence (Parsons & Sclater, 1977), the total surface subsidence amounts to ~2.3 km.

Without the eclogitizied oceanic plateau, the dynamic topography is only induced by the cold oceanic slabs (Model 2). The dynamic surface topography has a long-wavelength deflection in an EW direction, without extra surface tilting toward the GOM (Figure 4b). The surface in the western GOM gradually subsided to the maximum magnitude of ~0.8 km by ~45 Ma, and the total tectonic subsidence is only ~1.6 km (Figure 5), indicating that the surface deflection caused by the thermal buoyancy of the slab maybe insufficient to explain the observation in the GOM.

If the density increase in the Hess conjugate crust is less than 200 kg/m^3, such as 100 kg/m^3 (Model 3), the dynamic surface subsidence above the Hess conjugate also decreases (Figure S2a). We also test the case in which the subducted Shatsky conjugate undergoes eclogitization. Another localized surface low appears above the eclogitizied Shatsky conjugate in the continental interior (Figure S2b). The surface low passes across Wyoming at ~52 Ma and arrives at the location of Minnesota and Iowa by 0 Ma. The surface low above the conjugates gradually attenuates when the density anomalies sink to deeper depths. In the western GOM, the dynamic topography reduces by ~400 m over the last ~20 Myr.

The influence of the radial viscosity of the mantle and the phase change at 660 km depth are tested in Models 5 and 6. When the lower mantle viscosity in Model 1 is reduced by a factor of 2, the magnitude and

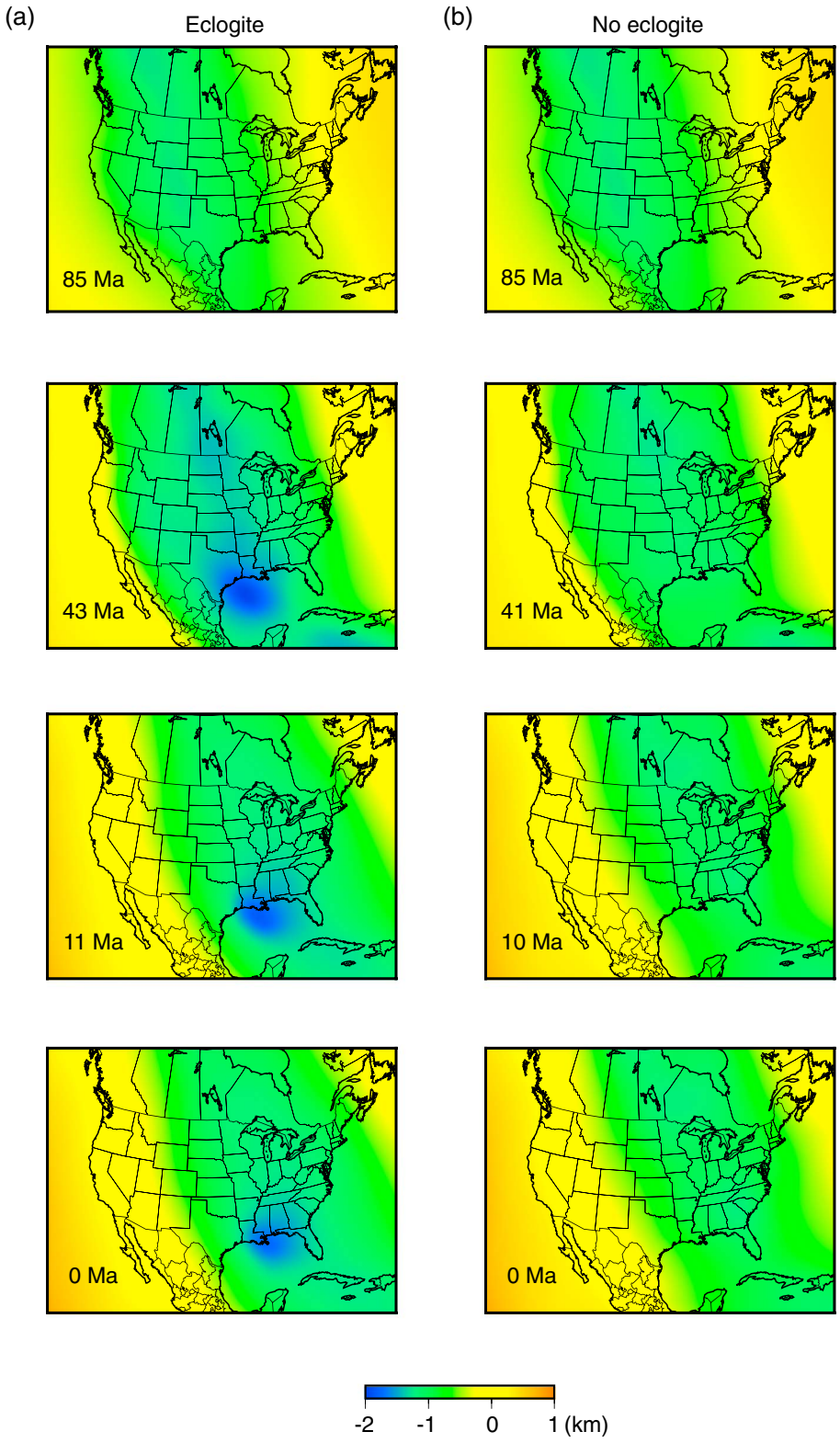

Figure 4. Dynamic topography at given ages. (a) Dynamic topography generated by both the low-temperature Farallon slab and the eclogitizied Hess conjugate. (b) Dynamic topography caused by the low-temperature Farallon slab only.

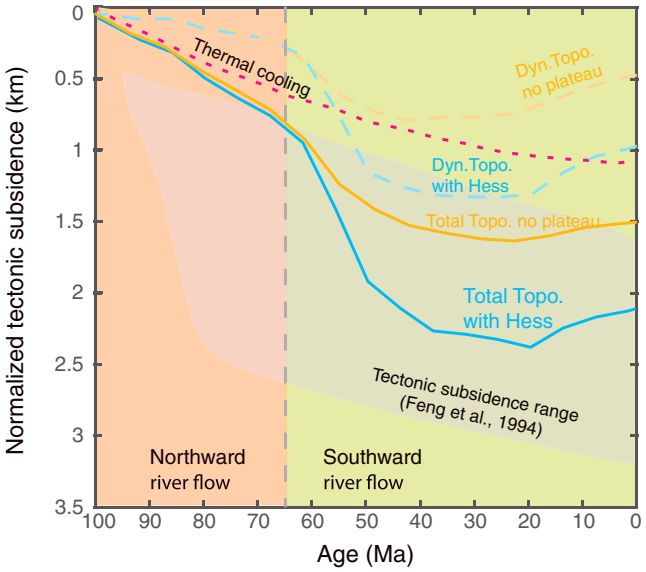

Figure 5. Average observed and predicted tectonic subsidence for boreholes A, B, and C (see Figure 1a for locations). The subsidence curves are normalized to a depth of zero at 100 Ma. The red dashed line shows theoretical thermal subsidence for a 50–150 Myr old oceanic crust (Parsons & Sclater, 1977). The grey shaded area is the tectonic subsidence range (Feng et al., 1994). The blue solid line is the total surface topography evolution, which is the sum of thermal subsidence (red dashed line) and predicted dynamic topography of Model 1 with the eclogitized Hess conjugate (blue dashed line). The yellow solid line is the sum of thermal subsidence and dynamic topography from Model 2 without eclogitized oceanic conjugates (yellow dashed line).

wavelength of the localized surface low increase moderately (Model 5; Figure S2c). Reducing the density jump at the 660 km discontinuity from 7% to 3.5% has little effect on the dynamic topography (Model 6; Figure S2d).

4. Discussion and Conclusions

The sedimentary record suggests an ~2 km subsidence in the GOM substantially after the rifting event (Feng et al., 1994). This enigmatic subsidence is within the framework of the continental-scale southward surface tilting and the eastward migration of the drainage system (Blum & Pecha, 2014; Galloway et al., 2011). Here we investigate the surface deflection caused by the negative buoyancy of an eclogitized oceanic plateau in addition to the low-temperature slab. The Hess conjugate subducted under northern Mexico and traveled below the northern GOM from ~68 Ma. A bull's-eye-shaped surface low with the maximum amplitude of ~1.8 km is generated above the eclogitized Hess conjugate. This localized surface low embeds within the large-scale smooth surface deflection produced by the low-temperature Farallon slab. Since ~55 Ma, the Hess conjugate migrated below the western GOM; as a result, the tectonic subsidence reaches a total depth of ~2.3 km (Figure 5).

The dense Hess conjugate also makes the GOM the lowest area on the dynamic topography map in North America. The timing of the predicted surface tilting toward the GOM induced by the Hess conjugate starting from the Cenozoic is coincident when the drainage system in southern North America started to routed sediments from the Western Cordillera to the Appalachian Mountains toward the GOM.

As the North American plate migrated westward over the subducted Farallon plate, the surface depression synchronously shifted eastward in the continental interior and the GOM. This could result in a broad eastward migration of river networks in North America (Figure 1a). The extra surface depression caused by the eclogitized Hess conjugate shifts along the northern GOM, which may determine the location where continental rivers empty into the GOM, and hence relocates the depocenter in the GOM eastward. Presently, the locus of deposition of the Mississippi river is located above the predicted position of the subducted Hess conjugate.

An eclogitized oceanic crust controls the extra surface low in the GOM. Eclogite is denser than pyrolite mantle in the upper mantle (Aoki & Takahashi, 2004). Perovskite transformation at the transition zone may make eclogite neutrally buoyant (e.g., Irifune & Ringwood, 1993) and traps the oceanic plate at the 660 km discontinuity (Anderson, 2007; Fukao et al., 2009). However, if the basaltic crust can penetrate the transition zone and transforms to a perovskitite at ~720 km depth, its density increases and becomes negatively buoyant again (e.g., Hirose et al., 1999 ; Ono et al., 2005). Numerous seismic studies show that the Farallon plate has penetrated into the lower mantle (e.g., Ritsema et al., 2011; Simmons et al., 2009; Van der Hilst et al., 1997). Presently, the residual topography (oceanic topography with normal thermal cooling removed) in eastern North America is negative, especially in the GOM, which is around −1 km (Hoggard et al., 2016; Winterbourne et al., 2014) (Figure 2). The long-lasting surface low in North America and the GOM indicates that the negative buoyancy persists in the Farallon plate and the Hess conjugate.

We investigate the surface expressions of the subducted Farallon plate and the Hess conjugate. Using a simple model with reasonable physical parameters, we predict the dynamic topography over North America, which is generally consistent with the observed broad surface deflection in the continental interior and the regional surface evolution in the GOM. We show that the surface topography mirrors the negative buoyancy and flow in the mantle. As the eclogitized Hess conjugate adds more negative buoyancy to the Farallon plate, the surface above the Hess conjugate experiences more subsidence. This could induce the surface tilting and guide the drainage system to flow southward, which established the GOM as the main sediment sink. The spatial-temporal correlations between the dynamic topography and the evolution of the GOM basin

demonstrate a substantial influence of mantle convection on this sedimentary basin, which could have implications for other mantle-convection-induced transient basins.

Acknowledgments
We thank Jolante van Wijk and Michelle Kominz for their thoughtful comments and suggestions. H.W. and M.G. have been supported by the National Science Foundation through EAR-1358646, EAR-1600956, and EAR-1645775 and by Statoil ASA. The original *CitcomS* code is obtained from Computational Infrastructure for Geodynamics (http://geodynamics.org).

References

Anderson, D. L. (2007). The eclogite engine: Chemical geodynamics as a Galileo thermometer. *Geological Society of America Special Papers*, *430*, 47–64.

Aoki, I., & Takahashi, E. (2004). Density of MORB eclogite in the upper mantle. *Physics of the Earth and Planetary Interiors*, *143*, 129–143.

Blum, M., & Pecha, M. (2014). Mid-Cretaceous to Paleocene North American drainage reorganization from detrital zircons. *Geology*, *42*(7), 607–610.

Bond, G. (1976). Evidence for continental subsidence in North America during the Late Cretaceous global submergence. *Geology*, *4*(9), 557–560.

Bower, D. J., Gurnis, M., & Flament, N. (2015). Assimilating lithosphere and slab history in 4-D Earth models. *Physics of the Earth and Planetary Interiors*, *238*, 8–22.

Cloos, M. (1993). Lithospheric buoyancy and collisional orogenesis: Subduction of oceanic plateaus, continental margins, island arcs, spreading ridges, and seamounts. *Geological Society of America Bulletin*, *105*(6), 715–737.

Coffin, M. F., & Eldholm, O. (1994). Large igneous provinces: Crustal structure, dimensions, and external consequences. *Reviews of Geophysics*, *32*, 1–36.

Cross, T. A., & Pilger, R. H. (1978). Tectonic controls of Late Cretaceous sedimentation, western interior, USA. *Nature*, *274*(5672), 653–657.

DeCelles, P. G. (2004). Late Jurassic to Eocene evolution of the Cordilleran thrust belt and foreland basin system, western USA. *American Journal of Science*, *304*(2), 105–168.

Feng, J., Buffler, R. T., & Kominz, M. A. (1994). Laramide orogenic influence on late Mesozoic-Cenozoic subsidence history, western deep Gulf of Mexico basin. *Geology*, *22*(4), 359–362.

Flament, N., Gurnis, M., Müller, R. D., Bower, D. J., & Husson, L. (2015). Influence of subduction history on South American topography. *Earth and Planetary Science Letters*, *430*, 9–18.

Flament, N., Gurnis, M., Williams, S., Seton, M., Skogseid, J., Heine, C., & Müller, R. D. (2014). Topographic asymmetry of the South Atlantic from global models of mantle flow and lithospheric stretching. *Earth and Planetary Science Letters*, *387*, 107–119.

Fukao, Y., Obayashi, M., Nakakuki, T., & Deep Slab Project Group. (2009). Stagnant slab: A review. *Annual Review of Earth and Planetary Sciences*, *37*, 19–46.

Galloway, W. E. (1989). Genetic stratigraphic sequences in basin analysis II: application to northwest Gulf of Mexico Cenozoic basin. *AAPG Bulletin*, *73*(2), 143–154.

Galloway, W. E. (2008). Depositional evolution of the Gulf of Mexico sedimentary basin. *Sedimentary Basins of the World*, *5*, 505–549.

Galloway, W. E., Whiteaker, T. L., & Ganey-Curry, P. (2011). History of Cenozoic North American drainage basin evolution, sediment yield, and accumulation in the Gulf of Mexico basin. *Geosphere*, *7*(4), 938–973.

Gurnis, M. (1992). Rapid continental subsidence following the initiation and evolution of subduction. *Science*, *255*(5051), 1556–1558.

Gurnis, M., Müller, R. D., & Moresi, L. (1998). Cretaceous vertical motion of Australia and the AustralianAntarctic discordance. *Science*, *279*(5356), 1499–1504.

Hacker, B. R. (1996). Eclogite formation and the rheology, buoyancy, seismicity, and H_2O content of oceanic crust. *Subduction Top to Bottom*, *337-346*.

Heller, P. L., & Liu, L. (2016). Dynamic topography and vertical motion of the US Rocky Mountain region prior to and during the Laramide orogeny. *Geological Society of America Bulletin*, *128*(5–6), 973–988.

Hirose, K., Fei, Y., Ma, Y., & Mao, H. K. (1999). The fate of subducted basaltic crust in the Earth's lower mantle. *Nature*, *397*(6714), 53–56.

Hoggard, M. J., White, N., & Al-Attar, D. (2016). Global dynamic topography observations reveal limited influence of large-scale mantle flow. *Nature Geoscience*, *9*(6), 456–463.

Irifune, T., & Ringwood, A. E. (1993). Phase transformations in subducted oceanic crust and buoyancy relationships at depths of 600–800 km in the mantle. *Earth and Planetary Science Letters*, *117*(1–2), 101–110.

Ko, J. Y., Helmberger, D., Wang, H., & Zhan, Z. (2017). Lower Mantle Substructure Embedded in the Farallon Plate: The Hess Conjugate. *Geophysical Research Letters*, *44*. https://doi.org/10.1002/2017GL075032

Korenaga, J., & Sager, W. W. (2012). Seismic tomography of Shatsky Rise by adaptive importance sampling. *Journal of Geophysical Research*, *117*, B08102. https://doi.org/10.1029/2012JB009248

Liu, L. (2014). Rejuvenation of Appalachian topography caused by subsidence-induced differential erosion. *Nature Geoscience*, *7*(7), 518–523.

Liu, L., Gurnis, M., Seton, M., Saleeby, J., Müller, R. D., & Jackson, J. M. (2010). The role of oceanic plateau subduction in the Laramide orogeny. *Nature Geoscience*, *3*(5), 353–357.

Liu, L., Spasojević, S., & Gurnis, M. (2008). Reconstructing Farallon plate subduction beneath North America back to the Late Cretaceous. *Science*, *322*(5903), 934–938.

Liu, S., & Nummedal, D. (2004). Late Cretaceous subsidence in Wyoming: Quantifying the dynamic component. *Geology*, *32*(5), 397–400.

Livaccari, R. F., Burke, K., & Şengör, A. M. C. (1981). Was the Laramide Orogeny related to subduction of an oceanic plateau? *Nature*, *289*(5795), 276–278.

Mitrovica, J. X., Beaumont, C., & Jarvis, G. T. (1989). Tilting of continental interiors by the dynamical effects of subduction. *Tectonics*, *8*, 1079–1094.

Nakanishi, M., Sager, W. W., & Klaus, A. (1999). Magnetic lineations within Shatsky Rise, northwest Pacific Ocean: Implications for hot spot-triple junction interaction and oceanic plateau formation. *Journal of Geophysical Research*, *104*, 7539–7556.

Ono, S., Ohishi, Y., Isshiki, M., & Watanuki, T. (2005). In situ X-ray observations of phase assemblages in peridotite and basalt compositions at lower mantle conditions: Implications for density of subducted oceanic plate. *Journal of Geophysical Research*, *110*, B02208. https://doi.org/10.1029/2004JB003196

Painter, C. S., & Carrapa, B. (2013). Flexural versus dynamic processes of subsidence in the North American Cordillera foreland basin. *Geophysical Research Letters*, *40*, 4249–4253. https://doi.org/10.1002/grl.50831

Parsons, B., & Sclater, J. G. (1977). An analysis of the variation of ocean floor bathymetry and heat flow with age. *Journal of Geophysical Research*, *82*, 803–827.

Pindell, J. L. (1985). Alleghenian reconstruction and subsequent evolution of the Gulf of Mexico, Bahamas, and Proto-Caribbean. *Tectonics*, *4*, 1–39.

Ritsema, J., Deuss, A. A., Van Heijst, H. J., & Woodhouse, J. H. (2011). S40RTS: A degree-40 shear-velocity model for the mantle from new Rayleigh wave dispersion, teleseismic traveltime and normal-mode splitting function measurements. *Geophysical Journal International*, *184*(3), 1223–1236.

Saleeby, J. (2003). Segmentation of the Laramide slab—Evidence from the southern Sierra Nevada region. *Geological Society of America Bulletin*, *115*(6), 655–668.

Salvador, A. (1991). Origin and development of the Gulf of Mexico basin. In *The Gulf of Mexico basin* (pp. 389–444). Washington, DC: Geological Society of America.

Simmons, N. A., Myers, S. C., Johannesson, G., & Matzel, E. (2012). LLNL-G3Dv3: Global P wave tomography model for improved regional and teleseismic travel time prediction. *Journal of Geophysical Research*, *117*, B10302. https://doi.org//10.1029/2012JB009525

Simmons, N. A., Myers, S. C., & Ramirez, A. (2009). *Multi-resolution seismic tomography based on recursive tessellation hierarchy (No. LLNL-PROC-414419)*. Livermore, CA: Lawrence Livermore National Laboratory (LLNL).

Smith, A. G., Smith, D. G., & Funnell, B. M. (1994). *Atlas of Mesozoic and Cenozoic coastlines* (99 pp.). New York: Cambridge University Press.

Spasojević, S., Liu, L., & Gurnis, M. (2009). Adjoint models of mantle convection with seismic, plate motion, and stratigraphic constraints: North America since the Late Cretaceous. *Geochemistry, Geophysics, Geosystems*, *10*, Q05W02. https://doi.org/10.1029/2008GC002345

Spasojević, S., Liu, L., Gurnis, M., & Müller, R. D. (2008). The case for dynamic subsidence of the US east coast since the Eocene. *Geophysical Research Letters*, *35*, L08305. https://doi.org/10.1029/2008GL033511

Sun, D., Gurnis, M., Saleeby, J., & Helmberger, D. (2017). A dipping, thick segment of the Farallon Slab beneath central US. *Journal of Geophysical Research: Solid Earth*, *122*, 2911–2928. https://doi.org/10.1002/2016JB013915

Vallier, T. L., Dean, W. E., Rea, D. K., & Thiede, J. (1983). Geologic evolution of Hess Rise, central North Pacific Ocean. *Geological Society of America Bulletin*, *94*(11), 1289–1307.

Van der Hilst, R. D., Widiyantoro, S., & Engdahl, E. R. (1997). Evidence for deep mantle circulation from global tomography. *Nature*, *386*, 578–584.

Winterbourne, J., White, N., & Crosby, A. (2014). Accurate measurements of residual topography from the oceanic realm. *Tectonics*, *33*, 982–1015. https://doi.org/10.1002/2013TC003372

Zhong, S., Zuber, M. T., Moresi, L., & Gurnis, M. (2000). Role of temperature-dependent viscosity and surface plates in spherical shell models of mantle convection. *Journal of Geophysical Research*, *105*, 11,063–11,082.